Glenoid Stress Distribution in Baseball Players Using Computed Tomography Osteoabsorptiometry: A Pilot Study

Running title: Glenoid Stress Distribution in Baseball Players

Tomohiro Shimizu MD, Norimasa Iwasaki MD, PhD, Kinya Nishida MD, PhD, Akio Minami MD, PhD, Tadanao Funakoshi MD, PhD (□□)

Department of Orthopaedic Surgery, Hokkaido University School of Medicine, Kita 15 Nishi 5 Kita-ku Sapporo, Hokkaido Japan 0608368

Abstract

Background It is important to understand the loading conditions when considering the pathology of shoulder disorders in overhead athletes. However, because throwing is a complicated motion, direct measurement of the stress distribution across the glenohumeral joint is difficult. Subchondral bone density reportedly reflects the cumulative stress acting on a joint surface under actual loading conditions.

Questions/Purposes To assess alterations in stress distribution across the glenoid cavity caused by pitching, we investigated the distribution of subchondral bone density in nonathletic volunteers and asymptomatic baseball players, including fielders and pitchers.

Methods We collected computed tomography (CT) imaging data from the dominant-side shoulder of 10 nonathletic volunteers (controls), 10 fielders, and 10 pitchers in a competitive college baseball league (all men aged 19–24 years, mean 20.7 years). We measured the distribution of subchondral bone density of the glenoid cavity using CT osteoabsorptiometry. The obtained stress distribution map was divided into four segments: anterosuperior, anteroinferior, posteroinferior, and posterosuperior regions. The location and percentages of high-density regions on the articular surface were analyzed quantitatively.

Results The percentages of high-density regions, including the anteroinferior, and posterior segments, were greater in pitchers and fielders than in controls. The percentages of high-density regions did not differ significantly between pitchers and fielders.

Conclusions The bicentric density patterns indicate that the cumulative force of pitching activity affects the long-term stress distribution across the glenoid cavity.

Clinical Relevance The current results provide useful information for analyzing pitching activity and clarifying the pathology of shoulder disorders associated with throwing.

Level of Evidence: Level II.

Introduction

A delicate balance between shoulder mobility and stability is required for throwing. Jobe et al. [10] identified shoulder instability as the primary abnormality in overhead throwers. Repetitive and excessive external rotation leads to tensile stressing of the anterior aspect of the shoulder capsule[13]. The shoulders of overhead athletes also reportedly have glenohumeral internal rotation deficits [2]. Burkhart et al. [2] proposed that an acquired loss of internal rotation caused by posteroinferior capsular contracture is the essential lesion leading to increased external rotation. A recent cadaveric model showed that the humeral head translates to a posterosuperior position during posterior capsular contracture [6]. Thus, throwing activities probably alter the cumulative forces and stress distributions. However, because of the difficulties in measuring these forces and stresses directly, the abnormal stress distributions across the shoulder joint associated with pitching activities has not been confirmed.

The pattern of subchondral bone density reportedly reflects the distribution of cumulative stresses acting on a joint surface under actual loading conditions [17]. Previous studies showed that a computed tomography (CT) osteoabsorptiometry method (CT-OAM) has potential for evaluating cumulative stress distribution patterns in shoulder joints [15, 19, 21, 22]. These studies found various stress distribution patterns in asymptomatic subjects [22], cuff tear shoulders [19], anterior glenohumeral instability [21], and symptomatic overhead throwers [15].

Therefore, the change in subchondral bone density may be one way to assess indirectly the stress distribution in the joints of asymptomatic overhead athletes.

The objectives in the current study were (1) to identify the distribution of subchondral bone density across the shoulder joint surface in nonathletic volunteers and asymptomatic baseball players, including fielders and pitchers, and (2) to assess alterations in the distribution of subchondral bone density associated with pitching activities.

Patients and Methods

We recruited 10 men who were nonathletic volunteers (control group: mean age, 22.4 years; range, 21–24 years), 10 men who were competitive baseball fielders (fielder group: mean age, 20.5 years; range, 19–22 years), and 10 men who were competitive baseball pitchers (pitcher group: mean age, 19.4 years; range, 19–20 years). We measured the passive glenohumeral range of motion in external and internal rotation at 90 degrees of shoulder abduction in the supine position with restriction of the scapulothoracic movement in the dominant and nondominant shoulders (Table 1). We presumed that the nondominant shoulders in high-level athletes would exhibit different stress distribution patterns compared with nonathletic subjects. Therefore, we selected nonathletic volunteers as the control group. No subjects had experienced any symptoms of disease in either shoulder within the past 3 years or had any history of shoulder trauma, although one pitcher had a history of reconstruction of the ulnar collateral ligament of the elbow. CT scans showed no apparently abnormal findings in any shoulder. All baseball players played in a competitive college league. They had participated in baseball since elementary school and had played the same position as at the time of the study since junior high school. We examined 26 right shoulders and four left shoulders. All subjects consented to participate in the study. The Institutional Review Board of our hospital approved this study.

The technical details of CT-OAM were as reported previously [8, 16, 19]. The observer who measured bone density was blinded to the group that each subject belongs to. We used a high-resolution (512 × 512 pixel matrix) helical CT scanner (CT High Speed Advantage; GE Medical Systems, Milwaukee, WI) to obtain axial images of the shoulder. The slice thickness and interval were set at 1 mm each, and the table speed was set at 1 mm per second. We transferred the image data to an image analyzing system (Advantage Windows; GE Medical Systems, Milwaukee, WI) and constructed true axial views at 1 mm intervals from a three-dimensional bone model. For further evaluation, we used a no commercial based, originally developed software program, (OsteoDens 4.0). In the axial image, the region of interest was manually selected so that it included the whole subchondral bone layer of the glenoid in all slices. After establishing the region of interest, we measured automatically in Hounsfield units (HU, defined as the X-ray attenuation whereby water is 0 and compact bone 1000) of the subchondral bone of the undersurface of the glenoid at each coordinate point at 1 mm intervals (Fig. 1). [25] The range of HU from 0 to 1800 was divided into nine equal intervals, and the measured HU at each coordinate point were mapped using a nine-grade color scale where red indicates the greatest bone density and deep blue indicates the lowest bone density. The measurement and mapping were repeated in each slice, and by stacking these data, a two-dimensional mapping image that projected the distribution of the subchondral bone density was obtained. At this point, the cortical bone at the peripheral area of the glenoid was included in the region of interest, because it was impossible to exclude the cortical bone area during the automatic measurement process. However, we carefully removed the cortical bone area from the target area of analysis during the next process, as described below.

Quantitative analysis of the mapping data focused on the location of high-density regions around the glenoid cavity. We defined the high-density region as a region of > 1200 HU (Grades 7- 9 on the nine-color scale) according to the previous reports [21, 22, 25]. We divided the glenoid cavity into four segments, beginning at 12 o'clock and proceeding clockwise to make four 90° segments: anterosuperior (AS), anteroinferior (AI), posteroinferior (PI), and posterosuperior (PS) (Fig. 2). We calculated the percentage of high-density region occupying each segment of the glenoid cavity and compared these statistically between segments within each group and between the three groups. We assessed intraobserver consistency in measuring of subchondral bone density by calculating the coefficient of variation within a region as the standard deviation divided by the mean value. For this assessment, we measured the HU five times on the same CT image. Statistical comparisons between groups and within each region were conducted using analysis of variance (ANOVA). We adjusted for multiple comparisons using Tukey's method. We performed statistical analyses using JMP 8.0 and SAS 9.2 (both SAS Institute, Cary, NC). The reliabilities between the observers and within each observer was calculated based on the intraobserver, interobserver, and residual variances estimated by the ANOVA table using Proc Mixed in SAS software. Intraobserver reproducibility was calculated on the basis of five consecutive measurements. Interobsever reliability was calculated from the measurements by two different orthopaedic surgeons. An intraclass correlation coefficient (ICC) of 1.0 represents perfect agreement and of 0 suggests that the measurements are entirely random. The appropriate intraobserver reproducibility depends on how one defines clinical agreement for the analysis. In this study, the reproducibility was considered acceptable for ICC value > 0.80.

Results

In the control group, the percentage occupied by the high-density region was significantly greater in the AS region than in the PS region in this group ($p = 0.008$, Fig.3). Bicentric density patterns were found across the glenoid cavity in the fielders and pitchers, but there were no obvious region-dependent differences (Table 2). All fielders and pitchers demonstrated a greater percentage and wider distribution of the high-density region in the anterior and posterior glenoid compared with the control group (Fig. 3).

The percentage of the high-density region in the total glenoid cavity were significantly greater in the fielder and pitcher groups ($p < 0.001$ and $p = 0.045$, respectively) than for the controls (Table 2). In fielders, the percentages of the high-density region in the AI, PI, and PS segments were also significantly greater ($p < 0.001$, $p < 0.001$, and $p = 0.002$, respectively) than in controls (Table 2). In pitchers, the percentages of the high-density region in the AI and PS segments were also significantly greater ($p = 0.012$ and $p = 0.02$, respectively) than in the control group (Table 2). The percentages of the high-density region of the AS segment did not differ significantly between any group. External rotation was significantly greater in the fielders and the pitchers ($p < 0.001$ and $p < 0.001$, respectively) than in the controls (Table 1). By contrast, internal rotation did not differ significantly between the baseball players and controls. The ICCs for intraobserver reliability and interobserver reproducibility were 0.90 (95% confidence interval, 0.84–0.96) and 0.80 (95% confidence interval, 0.74–0.86), respectively. The agreement for intraobserver and interobserver variations in the CT-OAM analysis was considered acceptable.

Discussion

Repetitive mechanical stress of the throwing motion affects both the static and dynamic stability of the shoulder. Although several biomechanical studies [6, 7, 13, 14]have reported on the mechanical stress, it is difficult to simulate the actual loading conditions of complicated pitching activity using cadaveric model. Therefore, we performed CT-OAM to predict the stress distribution across the glenoid cavity in baseball players and compared their results with those in nonathletic volunteers as a control group. The theoretical basis for the use of CT-OAM is that subchondral bone mineralization functionally adapts to repeated and long-term changes in the load on joints[17]. The advantage of CT-OAM is that it can be used to assess the long-term stress distribution without the need to reproduce the throwing motion. However, we also acknowledge that the distribution patterns that CT-OAM provides do not reflect the current condition of the athlete. Other advantages of this method are its reproducibility and high sensitivity[17]. In the current study, interobserver reliability and intraobserver reproducibility were relatively high.

Our study has several limitations. First, the results obtained were not based on direct measurement of the stresses on the shoulder joint, and we could not quantify the absolute joint stress. Although CT-OAM has potential for evaluating long-term stress distribution patterns, the distribution patterns do not reflect the current condition of the athlete. Second, the current results may reflect the overall bone quality but may not be specific to the throwing motion in the affected shoulder. To avoid the influence of individual bone quality, we included only men and matched the subjects' age between groups. Third, it is difficult to classify baseball players as only pitchers or fielders because most would have played both positions when younger and many of the throwing activities are similar in both positions. Finally, the sport of baseball involves both throwing and hitting motions, which are reflected in the differences in the stress distribution patterns in baseball players. To understanding better the loading conditions in pitching activities, further studies should analyze more data obtained from players with different skill levels and pitching forms, and of different ages.

We found that the percentages of high-density regions of the glenoid cavity, including the AI, PI, and PS segments, were greater in the asymptomatic baseball players than in the nonathletic volunteers. These bicentric high-density patterns reflect the long-term stress distribution across the glenoid cavity associated with playing baseball. The cumulative force in pitching activity would affect the stress distribution patterns. Fleisig et al.[5] reported that large loads are produced at the shoulder in the late cocking phase: 480 N of compressive force, 310 N of anterior shear force, and 250 N of superior shear force. After ball release, a maximum compressive force of 1090 N is generated at the shoulder and minimal shear force is generated in the anterior and inferior directions (80 and 100 N, respectively). Therefore, the large compression force at ball release would be an interesting focus for further investigation of the stress distribution pattern across the shoulder joint in baseball players. In our study, the high-density region was not found in the center of the glenoid as reported in a previous CT-OAM study [15]. Both the current results and the results reported [15] indicate that the compression force at ball release may not affect alteration the changes in bone density in the center of the glenoid, in contrast to our expectation based on biomechanical results. Although the magnitude of the compression force is very large, the distribution of subchondral bone density also depends on factors other than compression, such as tensile strength ,which is tangential to the articular surface[4]. In the late cocking phase, the high stress pattern in the AI segment of the glenoid cavity may be associated with tensile stress with AI microinstability and hyperlaxity. Schulz et al showed that the glenoid subchondral bone mineralization pattern in patients with anterior glenohumeral instability, indicated a more anterior and inferior stress distribution compared with people with stable shoulders [21]. We have no data on the link between the stress distribution pattern and the degree of translation of the glenohumeral joint, and this point needs to be in future work. By contrast, we found that the stress distributions in the PI and PS segments of the glenoid surface in the baseball-playing groups was greater than the control group. The greater range of external rotation in the baseball players compared with the nonathletic volunteers in our study is similar to that described previously [1, 11, 18, 23, 24]. Several other studies [3, 9, 12, 14, 20] reported that the rotator cuff encounters the posterior glenoid rim in the late cocking phase of baseball pitching. We consider that the excessive external rotation may reflect the bicentric stress pattern.

In this study, the percentage of the high-density region distribution around the glenoid surface did not differ between the pitchers and fielders. A previous report on stress distribution in the elbow found substantial differences between these athletes [16]. The inherent laxity and multiaxis nature of the shoulder explain the different results from those of the elbow joint. Another possibility is that the difference in the numbers of pitches did not affect the stress distribution as much as we expected. As we reported previously, various factors, such as pitching form and the athlete's skill level, should also be considered when studying the stress distribution. In addition, the influence of batting should not be ignored because batting activity is likely to affect the stress distribution across the glenoid cavity differently in the fielder compared with the pitcher, especially under the system of the designated hitter. The influence of each activity on the glenoid cavity should be clarified by further study.   CT-OAM can provide clinically useful information for analyzing individual loading conditions associated with pitching activities and for clarifying the pathology of shoulder disorders in overhead athletes. Further study may provide information that will enable the treating physician to predict whether an athlete is likely develop symptoms or remain asymptomatic shoulder prospectively. In conclusion, the percentages of the glenoid cavity occupied by high-density regions, especially in the AI, PI, and PS segments, were greater in asymptomatic baseball players, than in controls. These results indicate that these bicentric stress patterns across the glenoid surface reflect the activities of playing baseball, including throwing. We believe that CT-OAM is useful for obtaining information about the mechanical status of the glenohumeral joint in overhead athletes and for predicting the loading conditions in individual athletes. Prospective studies are needed to determine whether these athletes develop symptoms or maintain an asymptomatic shoulder.

Acknowledgments

We thank Koji Oba for statistical advice and Naomi Oizumi for advice about data analysis**.**

References

1. Brown LP, Niehues SL, Harrah A, Yavorsky P, Hirshman HP. Upper extremity range of motion and isokinetic strength of the internal and external shoulder rotators in major league baseball players. *Am J Sports Med.* 1988;16(6):577-585.
2. Burkhart SS, Morgan CD, Kibler WB. The disabled throwing shoulder: spectrum of pathology Part I: pathoanatomy and biomechanics. *Arthroscopy.* 2003;19(4):404-420.
3. Davidson PA, Elattrache NS, Jobe CM, Jobe FW. Rotator cuff and posterior-superior glenoid labrum injury associated with increased glenohumeral motion: a new site of impingement. *J Shoulder Elbow Surg.* 1995;4(5):384-390.
4. Eckstein F, Merz B, Schon M, Jacobs CR, Putz R. Tension and bending, but not compression alone determine the functional adaptation of subchondral bone in incongruous joints. *Anat Embryol (Berl).* 1999;199(1):85-97.
5. Fleisig GS, Andrews JR, Dillman CJ, Escamilla RF. Kinetics of baseball pitching with implications about injury mechanisms. *Am J Sports Med.* 1995;23(2):233-239.
6. Grossman MG, Tibone JE, McGarry MH, Schneider DJ, Veneziani S, Lee TQ. A cadaveric model of the throwing shoulder: a possible etiology of superior labrum anterior-to-posterior lesions. *J Bone Joint Surg Am.* 2005;87(4):824-831.
7. Huffman GR, Tibone JE, McGarry MH, Phipps BM, Lee YS, Lee TQ. Path of glenohumeral articulation throughout the rotational range of motion in a thrower's shoulder model. *Am J Sports Med.* 2006;34(10):1662-1669.
8. Iwasaki N, Minami A, Miyazawa T, Kaneda K. Force distribution through the wrist joint in patients with different stages of Kienbock's disease: using computed tomography osteoabsorptiometry. *J Hand Surg Am.* 2000;25(5):870-876.
9. Jobe CM. Posterior superior glenoid impingement: expanded spectrum. *Arthroscopy.* 1995;11(5):530-536.
10. Jobe FW, Kvitne RS, Giangarra CE. Shoulder pain in the overhand or throwing athlete. The relationship of anterior instability and rotator cuff impingement. *Orthop Rev.* 1989;18(9):963-975.
11. Johnson L. Patterns of shoulder flexibility among college baseball players. *J Athl Train.* 1992;27(1):44-49.
12. McFarland EG, Hsu CY, Neira C, O'Neil O. Internal impingement of the shoulder: a clinical and arthroscopic analysis. *J Shoulder Elbow Surg.* 1999;8(5):458-460.
13. Mihata T, Lee Y, McGarry MH, Abe M, Lee TQ. Excessive humeral external rotation results in increased shoulder laxity. *Am J Sports Med.* 2004;32(5):1278-1285.
14. Mihata T, McGarry MH, Kinoshita M, Lee TQ. Excessive glenohumeral horizontal abduction as occurs during the late cocking phase of the throwing motion can be critical for internal impingement. *Am J Sports Med.* 2010;38(2):369-374.
15. Mochizuki Y, Natsu K, Kashiwagi K, Yasunaga Y, Ochi M. Changes of the mineralization pattern in the subchondral bone plate of the glenoid cavity in the

shoulder joints of the throwing athletes. *J Shoulder Elbow Surg.* 2005;14(6):616-619.

16. Mommma D, Iwasaki N, Oizumi N, Nakatsuchi H, Funakoshi T, Kamishima T, Tadano S, Minami A. Long-term stress distribution patterns across the elbow joint in baseball players assessed by computed tomography osteoabsorptiometry. *Am J Sports Med.* 2011;39(2):336-341.
17. Muller-Gerbl M, Putz R, Hodapp N, Schulte E, Wimmer B. Computed tomography-osteoabsorptiometry for assessing the density distribution of subchondral bone as a measure of long-term mechanical adaptation in individual joints. *Skeletal Radiol.* 1989;18(7):507-512.
18. Myers JB, Laudner KG, Pasquale MR, Bradley JP, Lephart SM. Glenohumeral range of motion deficits and posterior shoulder tightness in throwers with pathologic internal impingement. *Am J Sports Med.* 2006;34(3):385-391.
19. Oizumi N, Suenaga N, Minami A, Iwasaki N, Miyazawa T. Stress distribution patterns at the coracoacromial arch in rotator cuff tear measured by computed tomography osteoabsorptiometry. *J Orthop Res.* 2003;21(3):393-398.
20. Paley KJ, Jobe FW, Pink MM, Kvitne RS, ElAttrache NS. Arthroscopic findings in the overhand throwing athlete: evidence for posterior internal impingement of the rotator cuff. *Arthroscopy.* 2000;16(1):35-40.
21. Schulz CU, Anetzberger H, Pfahler M, Refior HJ, Muller-Gerbl M. Anterior shoulder instability modifies glenoid subchondral bone density. *Clin Orthop Relat Res.* 2004(423):259-263.
22. Schulz CU, Pfahler M, Anetzberger HM, Becker CR, Muller-Gerbl M, Refior HJ. The mineralization patterns at the subchondral bone plate of the glenoid cavity in healthy shoulders. *J Shoulder Elbow Surg.* 2002;11(2):174-181.
23. Wilk KE, Meister K, Andrews JR. Current concepts in the rehabilitation of the overhead throwing athlete. *Am J Sports Med.* 2002;30(1):136-151.
24. Yamamoto N, Itoi E, Minagawa H, Urayama M, Saito H, Seki N, Iwase T, Kashiwaguchi S, Matsuura T. Why is the humeral retroversion of throwing athletes greater in dominant shoulders than in nondominant shoulders? *J Shoulder Elbow Surg.* 2006;15(5):571-575.
25. Zumstein V, Kraljevic M, Huegli R, Muller-Gerbl M. Mineralisation patterns in the subchondral bone plate of the humeral head. *Surg Radiol Anat.* 2011.

Legends

Fig. 1 The image shows how subchondral bone region of the glenoid cavity was identified automatically using customized software. In each oblique axial slice, we measured Hounsfield units of x-ray absorption in the subchondral bone at each coordinate point at 1 mm intervals. For quantitative analysis, the distribution pattern is represented as a surface-mapping image depicted by a nine-color scale.

Fig. 2 Image shows segments used for quantitative analysis of the bone density mapping data for the glenoid cavity: AS = anterosuperior, AI = anteroinferior, PI = posteroinferior, and PS = posterosuperior (PS).

Fig. 3 Graph shows distribution of subchondral bone density values across the articular surface of the glenoid cavity in each group.

Table 1. Characteristics of control and baseball players

Group	No.	Age (yr)	Dominant	At bat	Height (cm)	Weight (kg)	Dominant ER	Dominant IR	Nondominant ER	Nondominant IR	Comment
Control	1	21	right	NA	173	65	95	40	90	35	
	2	22	left	NA	173	65	100	30	100	30	
	3	22	right	NA	174	54	95	35	90	45	
	4	22	right	NA	167	63	100	35	90	40	
	5	22	right	NA	175	71	120	40	90	50	
	6	24	right	NA	172	72	100	35	90	35	
	7	23	right	NA	187	95	95	45	90	30	Right clavicle fracture
	8	23	right	NA	178	61	105	35	105	50	Left radius fracture
	9	24	right	NA	178	62	115	35	95	50	
	10	21	right	NA	169	65	100	40	90	40	
Mean		22.4			175	67	103	37	93	41	
Fielder	1	22	right	left	167	62	120	50	115	55	
	2	21	left	left	180	70	135	50	125	70	
	3	20	right	right	180	72	125	30	100	25	
	4	20	right	left	179	85	120	40	100	50	Right elbow pain (elementary school)
	5	22	right	right	171	59	130	35	95	50	Pitcher in elementary school
	6	22	right	right	179	80	120	30	100	45	
	7	21	right	left	174	68	150	30	110	40	
	8	19	right	right	174	64	115	30	90	35	
	9	19	right	left	178	80	120	40	115	60	Lumber disk herniation
	10	19	right	right	173	80	120	40	105	45	Right MCL of elbow reconstruction
Mean		20.5			176	72	126	38	106	48	
Pitcher	1	19	right	right	183	83	130	45	105	60	Right cubital tunnel syndrome

2	20	left	left	176	73	120	30	90	30	L5 spondylothesis
3	20	left	left	186	80	120	30	110	30	Left tibia fracture
4	19	right	right	180	81	140	45	115	70	Left ankle operation
5	20	right	right	180	71	110	45	90	50	
6	19	right	right	180	70	125	45	95	55	
7	19	right	right	177	71	110	30	95	40	
8	19	right	right	191	88	130	40	110	40	
9	20	right	right	185	70	125	45	100	50	Left clavicle fracture
10	19	right	right	174	70	140	30	130	60	
Mean	19.4			181	76	125	39	104	49	

ER = external rotation; IR = internal rotation; MCL = medial collateral ligament.

Table 2. Mean percentage of high density in each region in controls, fielders, and pitchers

Group	Control (mean ± SD)	Fielder (mean ± SD)	Pitcher (mean ± SD)	C vs F	C vs P	F vs P
Anterosuperior glenoid	26.4 ± 4.5	31.6 ± 3.2	21.3 ± 3.9	0.586	0.642	0.158
Anteroinferior glenoid	13.3 ± 3.3	45.0 ± 6.0	36.7 ± 6.1	< 0.001	0.012	0.513
Posteroinferior glenoid	15.8 ± 3.9	42.4 ± 4.7	29.5 ± 4.9	< 0.001	0.092	0.125
Posterosuperior glenoid	9.0 ± 1.9	30.0 ± 2.4	24.9 ± 5.9	0.002	0.020	0.598
Total surface glenoid	16.8 ± 2.7	37.8 ± 2.4	28.3 ± 4.0	< 0.001	0.045	0.108

C = Control; F = Fielder; P = Pitcher.

Figure 1

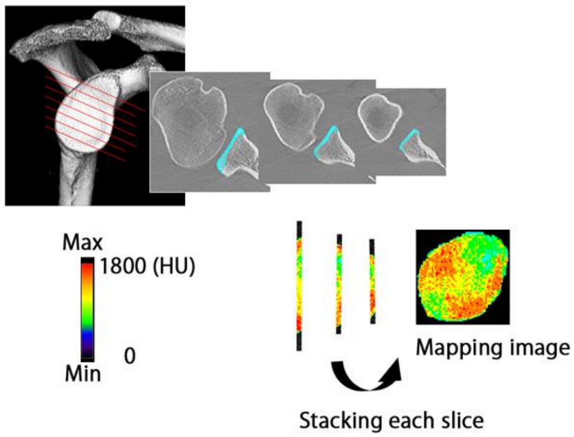

Figure 2

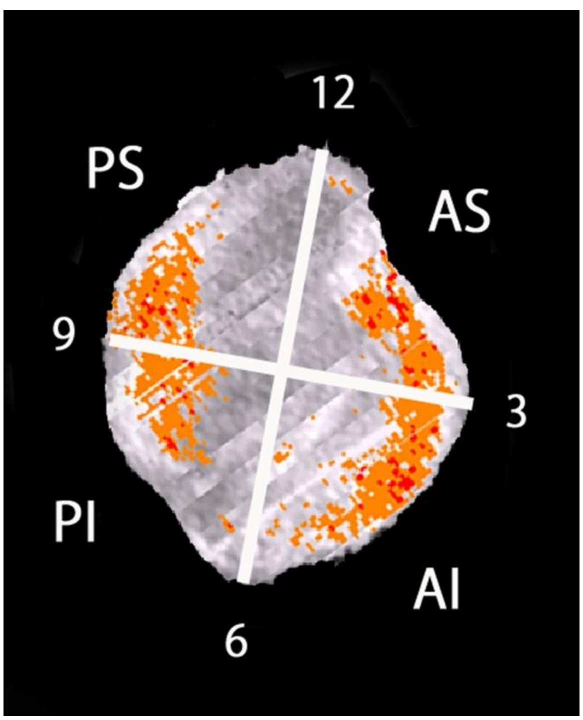

Figure 3